A Comparative Study of Formulations and Algorithms for Reliability-Based Co-Design Problems

Tonghui Cui

Department of Industrial and Enterprise Systems
Engineering,
University of Illinois at Urbana-Champaign,
Urbana, IL 61801
e-mail: tcui3@illinois.edu

James T. Allison

Department of Industrial and Enterprise Systems
Engineering,
University of Illinois at Urbana-Champaign,
Urbana, IL 61801
e-mail: jtalliso@illinois.edu

Pingfeng Wang

Department of Industrial and Enterprise Systems
Engineering,
University of Illinois at Urbana-Champaign,
Urbana, IL 61801
e-mail: pingfeng@illinois.edu

While integrated physical and control system co-design has been demonstrated successfully on several engineering system design applications, it has been primarily applied in a deterministic manner without considering uncertainties. An opportunity exists to study non-deterministic co-design strategies, taking into account various uncertainties in an integrated co-design framework. Reliability-based design optimization (RBDO) is one such method that can be used to ensure an optimized system design being obtained that satisfies all reliability constraints considering particular system uncertainties. While significant advancements have been made in co-design and RBDO separately, little is known about methods where reliability-based dynamic system design and control design optimization are considered jointly. In this article, a comparative study of the formulations and algorithms for reliability-based co-design is conducted, where the co-design problem is integrated with the RBDO framework to yield solutions consisting of an optimal system design and the corresponding control trajectory that satisfy all reliability constraints in the presence of parameter uncertainties. The presented study aims to lay the groundwork for the reliability-based co-design problem by providing a comparison of potential design formulations and problem-solving strategies. Specific problem formulations and probability analysis algorithms are compared using two numerical examples. In addition, the practical efficacy of the reliability-based co-design methodology is demonstrated via a horizontal-axis wind turbine structure and control design problem.

[DOI: 10.1115/1.4045299]

Keywords: design automation, design optimization, reliability in design, systems design, uncertainty analysis

1 Introduction

Dynamic systems are common subjects of engineering design. The behavior of time-varying system states depends both on plant (physical system) and controller design decisions. These state trajectories affect the activity of path and boundary constraints. Moreover, constraints that are inactive under deterministic treatment may become active when accounting for various sources of uncertainty. To meet engineering system requirements, system designers may formulate an optimization problem with chance constraints that enforce feasibility with a desired level of reliability with respect to both plant and controller design decisions.

The above problem fits into the broad discipline of multidisciplinary design optimization (MDO) with probabilistic constraints. It consists of three parts: plant design, controller design, and reliability assessment. Plant design concerns decisions regarding the embodiment of the physical aspects of a system. Controller design relates to the sensing and regulating of dynamic system behavior by providing proper control inputs. Reliability assessment evaluates the probability of system failure considering various sources of uncertainty. The two major classes of uncertainty are aleatory and epistemic, where the former comes from the random nature of parameters, and the later is usually due to lack of

information. The uncertainty-based co-design problem has been addressed partially by two types of previous studies, namely, co-design and uncertainty-based design optimization. Co-design is a special class of MDO problems where the coupled design disciplines include plant (physical system) and control system design [1]. Unlike conventional sequential design methods, where control design is performed after plant design is complete, co-design is an integrated approach that accounts fully for design coupling between plant and control design, producing a systemoptimal result [2]. Some researchers have studied the simulationbased implementation of co-design. Fathy et al. showed the successful implementation of nested co-design for a passive/ active automotive suspension system [3]. Yan and Yan demonstrated the improved performance of a four-bar linkage powered by a variable-speed servo motor [4]. Allison et al. demonstrated the application of both simultaneous and nested co-design for a robotic manipulator [5], an active suspension [6], and horizontalaxis wind turbines [7].

Co-design methods presented so far in the literature have been applied primarily in a deterministic manner. Developing non-deterministic co-design strategies, including the incorporation of uncertainty-induced failures into an integrated co-design framework, may help to reach a reliable and system-optimal design of an actively controlled dynamical system. Simply applying a safety factor to account for uncertainty not only limits performance but may not adequately account for multiple constraints and complex uncertainty propagation in a way that ensures reliable performance. Uncertainty-induced failures can be quantified as the probability of failure, which are included in standard RBDO formulations. Various strategies have been presented in the literature to

¹Corresponding author.

Contributed by the Design Automation Committee of ASME for publication in the JOURNAL OF MECHANICAL DESIGN. Manuscript received June 16, 2019; final manuscript received October 18, 2019; published online October 25, 2019. Assoc. Editor: Nam H. Kim.

evaluate the probability of failure efficiently. For example, Tu et al. presented a general probabilistic constraint evaluation for RBDO and compared the performance of the reliability index approach (RIA) and performance measurement approach (PMA) [8]. A hybrid mean value method was introduced to handle concave problems for the slow convergence of the conjugate mean value method, and a modified version was proposed to handle nonlinearities in Refs. [9,10]. To compare several first-order approximate methods, Chiralaksanakul and Mahadevan compared their efficiency, accuracy, and convergence through numerical examples [11]. In the case of correlated inputs, Noh et al. provided a method that converts dependent input variables to independent standard normal variables using the Gaussian copula [12]. The studies described above all use double-loop formulations, where design optimization (DO) and reliability analysis (RA) are nested. Likewise, single-loop methods [13,14] and decoupled methods [15] have also been proposed to reduce the computational burden.

While significant advancements have been made recently in co-design and RBDO separately, limited work has been done to combine reliability-based dynamic system design and control design optimization. Here, we seek to capitalize on integrated plant and control design to enhance system reliability, supporting system-optimal performance while satisfying reliability constraints. To the authors' best knowledge, RBDO has not yet been applied to co-design problems to address design uncertainties. A unified approach to combining co-design and RBDO could lead to reliable optimal solutions, with reasonable solution cost. This paper serves as an initial attempt to solve co-design problems with an efficient RBDO method.

Note that other formulations exist for uncertainty-based design optimization, including dynamic systems. One example is robust design optimization (RDO), which seeks to optimize the mean design performance as well as minimize the influence of variations in design variables. An initial implementation of RDO for co-design problems is discussed in Ref. [16], where Azad and Alexander-Ramos show a simultaneous design of the plant and controller by including robustness terms in both the objective function and the inequality constraints. In their formulation, the robustness terms are related to the first-order Taylor series approximation of the variance-induced functional variation. For a general MDO problem with uncertainties, a comparative study of RBDO, possibility-based design optimization, and RDO was presented by Park et al. [17]. It was shown by these authors that RDO suffers from its complex problem formulation and that RBDO can provide a good estimate of system reliability if sufficient samples are available.

This article involves three primary contributions. First, general formulations of reliability-based co-design problems are provided, including both simultaneous and nested variants. These formulations are specifically limited to consideration of only plant parameter uncertainties. A more general and unified treatment of multiple sources of uncertainty is a topic of ongoing work. Second, a feasible simplification of the inner loop is proposed to improve the computational solution efficiency of the proposed nested structure. Third, implementation and parametric studies of these formulations, based on both numerical and engineering examples, provide quantitative insights into the formulation and solution characteristics in terms of efficacy, accuracy, efficiency, and robustness. In summary, this article addresses the initial implementation of RBDO for co-design problems, in the presence of aleatory design uncertainties.

The rest of this article is organized into four parts: Sec. 2 introduces concepts and methods for co-design and RBDO. Section 3 provides details regarding reliability-based co-design (RBCD) problem formulation and outlines the proposed method for solving this class of problem under aleatory uncertainties. Two numerical examples and one design application (simplified co-design of a wind turbine supported by a truss tower) are presented in Sec. 4. Finally, Sec. 5 concludes the paper and describes future opportunities for related studies.

2 Background

This section introduces the background required for RBDO co-design with aleatory uncertainty. Optimal control is an important component of co-design and is discussed briefly. This is followed by a brief discussion of co-design problem formulations and solution strategies. Finally, a review of RBDO is provided, specifically to motivate its use as one possible technique to formulate co-design problems with uncertainties.

2.1 Optimal Control Problem. An optimal control problem concerns optimization of a control system, which involves control inputs that evolve over time and influence the behavior of a dynamic system that often is characterized by a set of by ordinary differential equations (ODEs):

$$\dot{\boldsymbol{\xi}} - \mathbf{f}(t, \boldsymbol{\xi}(t), \mathbf{x}_c(t)) = \mathbf{0}$$

$$\boldsymbol{\xi}(t_0) = \boldsymbol{\xi}_0$$
 (1)

where $\xi(t)$ is the set of state trajectories, $\mathbf{x}_c(t)$ is the control input, t is the time, and ξ_0 is the initial state at the initial time t_0 . In a direct optimal control problem, we seek to minimize a cost function that depends on dynamic system behavior, with respect to the infinite-dimensional control input trajectories $\mathbf{x}_c(t)$. An example of a cost function over a finite time horizon is

$$J(\mathbf{x}_c(t)) = \int_{t_0}^{t_f} L(t, \boldsymbol{\xi}(t), \mathbf{x}_c(t)) dt + R(t_f, \boldsymbol{\xi}_f)$$
 (2)

where $L(\cdot)$ defines the running cost and $R(\cdot)$ defines the cost of reaching a specific final state ξ_f at the final time t_f [18].

Optimal control problems may include several types of constraints, including time-independent constraints, inequality path constraints that limit the state and control trajectories, and boundary conditions that define the initial and final states (e.g., for periodic optimal control). In co-design, system performance is optimized not only with respect to control input design but also with respect to physical system design.

2.2 Co-Design Problem Formulation. Co-design problems address directly the design coupling between the plant and control design decisions. Design coupling is distinct from physics coupling, but often the latter gives rise to the former. Consider a design optimization problem with two or more sets of design variables (e.g., plant and control). Design coupling exists between two sets of variables if changes in one set influence how design decisions should be made in the other set (e.g., optimal control decisions depend on plant design). In realistic co-design problems, bi-directional design coupling exists between plant and control design, and conventional sequential design methods cannot account fully for this coupling. Achieving system optimality requires a simultaneous variation of both sets of variables (or approaches that are mathematically equivalent to simultaneous plant and control design) [1]. One approach to expressing the simultaneous co-design formulation is

$$\begin{aligned} & \min_{\mathbf{x}_{p}, \, \mathbf{x}_{c}(t), \, \boldsymbol{\xi}(t)} & \theta \left(t, \, \boldsymbol{\xi}(t), \, \mathbf{x}_{c}(t), \, \mathbf{x}_{p} \right) \\ & \text{subject to} & \dot{\boldsymbol{\xi}} - \mathbf{f} \left(t, \, \boldsymbol{\xi}(t), \, \mathbf{x}_{c}(t), \, \mathbf{x}_{p} \right) = \mathbf{0} \\ & & \mathbf{G} \left(t, \, \boldsymbol{\xi}(t), \, \mathbf{x}_{c}(t), \, \mathbf{x}_{p} \right) \leq \mathbf{0} \end{aligned} \tag{3}$$

where \mathbf{x}_p is the vector of physical system design variables. The equality constraint $\mathbf{f}(\cdot)$ enforces system dynamics. Here, adjustments to plant design (\mathbf{x}_p) provide additional degrees of design freedom beyond control design. The inequality constraints $\mathbf{G}(\cdot)$ enforce requirements such as physical failure modes. These in general are path constraints but may also be time-independent. Here, $\theta(\cdot)$ represents a general cost function that may depend on time, state, control, and plant design. It should be noted here that

when the control trajectories $\mathbf{x}_c(t)$ are treated directly as optimization variables, this is known as open-loop optimal control (OLOC). OLOC problems are especially effective at identifying system performance limits at early design phases, but most real systems require closed-loop control (CLC), which may have different limitations when compared with OLOC [19]. Later-stage co-design studies should account for practical implementation considerations for the closed-loop control.

This simultaneous formulation a bove is the fundamental integrated design problem [20]. It is often desirable to identify mathematically equivalent problem formulations that yield system optimality, but that also support easier numerical solution. One such strategy is to use the nested co-design formulation, which adopts a nested structure that optimizes plant design in an outer loop, and for every candidate plant design, the best possible performance is determined by solving an inner-loop optimal control problem. The outer-loop formulation is [1,21]

$$\min_{\mathbf{x}_{p}} \qquad \qquad \boldsymbol{\theta}\left(t, \boldsymbol{\xi}_{*}(t), \mathbf{x}_{c*}(t), \mathbf{x}_{p}\right) \\
\text{subject to:} \qquad \mathbf{G}_{O}\left(\mathbf{x}_{p}\right) \leq \mathbf{0} \\
\qquad \qquad \mathbf{G}_{F}\left(\mathbf{x}_{p}\right) \leq \mathbf{0}$$

where $\mathbf{x}_{c^*}(t)$ and $\boldsymbol{\xi_*}$ refer to the optimal control and the corresponding state trajectories determined by the inner loop. $\mathbf{G}_O(\cdot)$ represents the constraints that depend on the plant design variables only. The additional constraint $\mathbf{G}_F(\cdot)$ is called the feasibility constraint here. The purpose of including a feasibility constraint is to limit the plant design space such that the corresponding feasible control space is non-empty. As indicated in Ref. [21], a proper feasibility constraint, though possibly difficult to find, renders the control subproblem well-posed for gradient-based methods.

The inner-loop problem is a typical optimal control problem. For the nested co-design structure, it is formulated as

$$\min_{\mathbf{x}_{c}(t), \, \boldsymbol{\xi}(t)} \qquad \qquad \theta \left(t, \, \boldsymbol{\xi}(t), \, \mathbf{x}_{c}(t), \, \mathbf{x}_{p} \right)$$
subject to:
$$\dot{\boldsymbol{\xi}} - f \left(t, \, \boldsymbol{\xi}(t), \, \mathbf{x}_{c}(t), \, \mathbf{x}_{p} \right) = \mathbf{0}$$

$$\mathbf{G}_{I} \left(t, \, \boldsymbol{\xi}(t), \, \mathbf{x}_{c}(t), \, \mathbf{x}_{p} \right) \leq \mathbf{0}$$
(5)

The plant design variables \mathbf{x}_p remain fixed while solving the inner-loop problem. The inner-loop constraints include the dynamics $\mathbf{f}(\cdot)$ and inner-loop inequality constraints $\mathbf{G}_I(\cdot)$. Compared to the simultaneous strategy, the nested strategy can both utilize existing efficient optimal control methods and decouple the optimal control problem from the complication of plant design. Application of solution methods tailored for optimal control often results in a net computational benefit for the nested approach, but not always. A detailed discussion regarding the optimality conditions using analytic solutions to Pontryagin's maximum principle (PMP) [22] can be found in Ref. [23] for both simultaneous and nested formulations.

There are, in general, two classes of methods to solve the optimal control problem: (1) optimize-then-discretize methods and (2) discretize-then-optimize methods. The former is sometimes referred to as indirect optimal control methods and the latter as direct optimal control methods. Optimize-then-discretize (indirect) methods work by applying optimality conditions to the optimal control problem to form a boundary-value problem (BVP). For example, PMP provides necessary optimality conditions and Hamilton–Jacobi–Bellman equation, which provides a necessary and sufficient condition for optimality. In some cases, the resulting BVP has a closed-form solution (e.g., linear-quadratic regulator problems), but in general is solved numerically.

The second class of optimal control solution methods (discretize-then-optimize, or direct) work by transcribing the infinite-dimensional optimal control problem into a finite-dimension nonlinear program via time discretization of state and control trajectories. The system dynamics constraints ($\mathbf{f}(\cdot)$) are transformed from a system of ordinary differential equations into a set of algebraic

constraints when performing this discretization. Direct transcription (DT) is one class of discretize-then-optimize methods that has proven to be particularly effective for co-design, either for nested or simultaneous formulations. With proper meshing, the co-design problem can be solved accurately and efficiently [1]. For this reason, DT [23,24] is chosen here for inner-loop problems that require numerical solution (namely, the wind turbine case study).

Note that the current state-of-the-art co-design methods produce control solutions in the form of open-loop control (OLC) trajectories, which can reveal important insights for early-stage design studies. However, OLC is not practical for direct implementation in many systems, which instead require closed-loop control. In practice, due to information and physical limits, there is a gap in performance between the optimal OLC trajectory and the closestperforming CLC design. It has been suggested that the established OLC co-design methods could be integrated with system architecture decisions and detailed CLC design [19], but this is a challenging problem that remains a topic of ongoing work. In practice, OLC co-design results can be analyzed to inform CLC design, and performance improvements can be realized when compared with traditional sequential design approaches, but the resulting implementable system cannot be said to be system-optimal with respect to all design decisions.

2.3 Reliability-Based Design Optimization. Reliabilitybased design optimization (RBDO) replaces deterministic constraints with corresponding chance constraints. These constraints show dependency both on the design variables and their distributions; thus, they must be evaluated using reliability analysis. There are several strategies for RBDO formulation, such as doubleloop RBDO [8], decoupled RBDO [15], single-loop RBDO [13], and metamodel-based RBDO [25]. A double-loop strategy is used to solve the RBDO problem in this article, utilizing a nested strategy for reliability analysis and design optimization. Using a chanceconstrained feasibility constraint in the outer loop of the nested co-design problem and the approximated inner-loop reliability constraint of the proposed simplified formulation, however, utilizes similar ideas to decoupled RBDO, where reliability constraints are approximated by linearization. Three approaches exist for double-loop RBDO: the reliability index approach (RIA), the PMA, and the approximate moment approach. Details regarding these three approaches are reviewed in Ref. [26]. For this work, PMA and RIA are considered. Monte Carlo Simulation (MCS), a computationally expensive but accurate reliability analysis method, is utilized for benchmark comparison.

If a design problem has a design vector with uncertain variables $\mathbf{X} = (X_1, ..., X_{Nd})$ with a mean design vector $\mathbf{d} = (d_1, ..., d_{Nd}) = \boldsymbol{\mu}(\mathbf{X})$, the RBDO problem can be formulated as follows [26]:

$$\min_{\mathbf{d}} \qquad \theta(\mathbf{d})$$
subject to $Pr(G_j(\mathbf{X}, \mathbf{d}) \le 0) \ge \Phi(\beta^i), \ j = 1, \dots, N_c$

$$d_i^L \le d_i \le d_i^U, \ i = 1, \dots, N_d \qquad (6)$$

where N_d and N_c are the number of design variables and constraints, respectively, $G_f(\cdot)$ is the jth constraint, Φ is the cumulative distribution due to the standard normal distribution, β^I is the target reliability level, and d_i^L and d_i^U are the lower and upper bounds of the ith design variable. We further define F_{G_j} as the CDF of $G_f(\cdot)$ such that

$$F_{G_i} = Pr(G_j(\mathbf{X}, \mathbf{d}) \le 0) \tag{7}$$

For RIA, Eq. (6) can be rewritten as

$$\begin{aligned} & \underset{\mathbf{d}}{\min} & & \boldsymbol{\theta}(\mathbf{d}) \\ & \text{subject to} & & G_j^r = \beta^i - \Phi^{-1} \big(F_{G_j} \leq 0 \big) \\ & & & = \beta^i - \beta_j^s \leq 0, \ j = 1, \dots, N_c \\ & & & & d_i^L \leq d_i \leq d_i^U, \ i = 1, \dots, N_d \end{aligned} \tag{8}$$

The probability in RIA can be approximated using the first-order reliability method (FORM), which estimates the distance from the origin to the most probable point (MPP) in the *U*-space. For normal random variables, the *U*-space is simply the normalized distribution defined by its mean and standard deviation. The MPP can be found through the Hasofer-Lind and Rackwitz-Fiessler (HL-RF) method, which uses the steepest ascent direction of the constraint function to update the search point. Likewise, the RBDO problem using PMA can be formulated as follows:

$$\min_{\mathbf{d}} \qquad \theta(\mathbf{d})$$
subject to $G_j^p = F_{G_j}^{-1}(\Phi(\beta^i)) \le 0, j = 1, \dots, N_c$

$$d_i^L \le d_i \le d_i^U, i = 1, \dots, N_d$$
(9)

Here, $F_{G_j}^{-1}$ represents the inverse transformation. To solve for G_j^p , the first-order estimate is obtained by solving the following optimization problem in the *U*-space:

$$\max_{\mathbf{U}} \qquad g_j(\mathbf{U})$$
subject to $\|\mathbf{U}\| = \beta^t$

where the constraint in the above problem defines the target reliability surface. The MPP, \mathbf{u}_j^* , is the point on the target reliability surface that maximizes the constraint function in the *U*-space $g_j(\cdot)$, where $g_j(\mathbf{u}) \equiv G_j(\mathbf{X}(\mathbf{u}))$.

The method used to find the MPP when applying PMA in the studies presented here is the advanced mean value (AMV) method. The initial estimate using AMV is calculated as follows [27]:

$$\mathbf{u}^{(0)} = \beta^t \mathbf{n}^{(0)} = \beta^t \frac{\nabla_{\mathbf{U}} G_j(\mathbf{u} = 0)}{\|\nabla_{\mathbf{U}} G_j(\mathbf{u} = 0)\|}$$
(11)

where $\mathbf{u} = 0$ corresponds to the mean values of \mathbf{x} and $\mathbf{n}^{(k)}$ is the steepest descent direction at the MPP of the kth iteration. The MPP is updated as follows:

$$\mathbf{u}^{(k+1)} = \beta^t \mathbf{n}^{(k)} = \beta^t \frac{\nabla_{\mathbf{U}} G_j(\mathbf{u}^{(k)})}{\|\nabla_{\mathbf{U}} G_j(\mathbf{u}^{(k)})\|}$$
(12)

Typically, both the RIA and the PMA methods can easily estimate a target reliability for common distribution types. However, the RIA tends to diverge for distributions other than the normal distribution, whereas PMA does not show dependency on the distribution. Also, PMA outperforms RIA in a sense of reliability analysis convergence for its robustness and efficiency. RIA and PMA are both firstorder reliability methods (FORM). In cases where constraints (or limit state functions) are highly nonlinear, it is desirable to consider the curvature of constraints using second-order reliability methods. Other RBDO methods, such as single-loop methods and decoupled methods, can potentially be implemented to improve the efficiency of overall problem solution. Using the single-loop methods, however, can cause inaccuracy due to an approximated MPP, while the efficiency improvement of decoupled methods is questionable since it increases the number of outer-loop iterations and increases computation time due to solving for additional optimal control trajectories in the inner loop. The trade-off for both scenarios are application dependent and therefore not included in the current work.

3 Reliability-Based Co-Design Optimization

Considering a controlled system with uncertainties in the plant design variables, the task is to find a feasible combination of plant design variable and control trajectory values that satisfies all constraints in the presence of design uncertainties. Other types of uncertainty, such as exogenous variables for the dynamic system, may be especially important for some systems, but are outside the scope of this initial RBCD formulation study. In this section, we will introduce several RBCD problem formulations and discuss detailed implementation strategies for solving this type of problem.

3.1 Simultaneous Formulation. The most straightforward RBCB formulation is the simultaneous co-design formulation with double-loop reliability analysis. Following the nomenclature from the earlier discussion, the problem with normally distributed random design variables $(\mu_{x_p}, \sigma_{x_p})$ can be formulated as follows:

$$\min_{\boldsymbol{\mu}_{x_p}, \mathbf{x}_c(t), \, \boldsymbol{\xi}(t)} \quad \boldsymbol{\theta} \Big(t, \, \boldsymbol{\xi}(t), \, \mathbf{x}_c(t), \, \boldsymbol{\mu}_{x_p} \Big)$$
subject to:
$$\dot{\boldsymbol{\xi}} - \mathbf{f} \Big(t, \, \boldsymbol{\xi}(t), \, \mathbf{x}_c(t), \, \boldsymbol{\mu}_{x_p} \Big) = \mathbf{0}$$

$$Pr \Big(\mathbf{G} \Big(t, \, \boldsymbol{\xi}(t), \, \mathbf{x}_c(t), \, \boldsymbol{\mu}_{x_p} \Big) \leq \mathbf{0} \Big) \geq \Phi \Big(\boldsymbol{\beta}^t \Big)$$

$$\boldsymbol{\mu}_{x_n}^{Lo} \leq \boldsymbol{\mu}_{x_n} \leq \boldsymbol{\mu}_{x_n}^{Up}$$

$$(13)$$

where the probability of failure can be evaluated using the FORM methods introduced in Sec. 2. Several simplifications are made to emphasize the basic characteristics, where only the objective function, the dynamic constraint, the probability constraint, and bounds for the mean design variables are present.

The main purpose of RBDO is generating feasible designs in the presence of uncertainties; thus, the objective is usually evaluated at the mean design variables. Objective function variance can also be included to emphasize robustness in design. This modification, however, is not necessary if the objective function is insensitive to the design variations and the design variation is small.

Other than the deterministic constraints that are not affected by design variations, two types of constraints are considered here: hard constraints and soft constraints. Hard constraints, usually physics-based, are always active regardless of design variations. For example, the dynamics can be evaluated at the mean design for control trajectory generation. For sample-based reliability analysis, the dynamics are updated with the sample designs. In contrast, activity of soft constraints is affected by the randomness in design variables (e.g., path constraints and boundary conditions). Within soft constraints, equality constraints can be reformulated as inequality constraints that are bounded from both sides, with a choice of acceptance level. Using this reformulation, we may consider a formulation using only soft inequality constraints for reliability analysis.

System states are time-dependent, which makes RA time-dependent also for a co-design problem. This brings in design complexity and evaluation difficulty since it requires numerical integration of a random process. For this work, a simulation-based method is applied as it evaluates the simulated sample performances and uses the classification result to estimate the probability of failure. This method may become impractical for expensive simulations. To improve the efficiency, several methods that convert time-dependent RA into time-independent ones had been proposed, such as extreme value-based methods [28–31], composite limit state methods [32], and out-crossing rate-based methods [33]. These methods can potentially improve the efficiency of co-design reliability analysis and are considered for future improvements.

3.2 Nested Formulation. An alternative to the simultaneous formulation is the nested formulation. Following Eqs. (4)–(5), the RBCD problem described in Eq. (13) can be formulated as a deterministic plant design problem in the outer loop, and

reliability-based optimal control design in the inner loop:

$$\min_{\boldsymbol{\mu}_{x_p}} \quad \theta \left(t, \, \boldsymbol{\xi}_*(t, \, \boldsymbol{\mu}_{x_p}), \, \mathbf{x}_{C*}(t, \, \boldsymbol{\mu}_{x_p}, \, \boldsymbol{\mu}_{x_p} \right) \\
\text{subject to} \quad \mathbf{G}_F \left(\boldsymbol{\mu}_{x_p} \right) \leq \mathbf{0} \\
\boldsymbol{\mu}_{x_p}^{Lo} \leq \boldsymbol{\mu}_{x_p} \leq \boldsymbol{\mu}_{x_p}^{Up}$$
(14)

where $\mathbf{x}_{\mathbf{c}*}(t, \boldsymbol{\mu}_{x_p})$ and $\boldsymbol{\xi}_{\bullet}(t, \boldsymbol{\mu}_{x_p})$ refer to the optimal control trajectory and the corresponding state trajectory determined by the inner loop, which is defined in Eq. (15):

$$\min_{\mathbf{x}_{c}(t), \, \boldsymbol{\xi}(t)} \quad \theta\left(t, \, \boldsymbol{\xi}(t, \, \boldsymbol{\mu}_{x_{p}}), \, \mathbf{x}_{c}(t, \, \boldsymbol{\mu}_{x_{p}}), \, \boldsymbol{\mu}_{x_{p}}\right)$$
subject to
$$\dot{\boldsymbol{\xi}} - \mathbf{f}\left(t, \, \boldsymbol{\xi}(t), \, \mathbf{x}_{c}(t), \, \boldsymbol{\mu}_{x_{p}}\right) = \mathbf{0}$$

$$Pr\left(\mathbf{G}\left(t, \, \boldsymbol{\xi}(t), \, \mathbf{x}_{c}(t), \, \boldsymbol{\mu}_{x_{p}}\right) \leq \mathbf{0}\right) \geq \Phi(\beta^{t})$$

Here, the feasibility constraint $G_F(\cdot)$ must enforce non-emptiness of inner-loop reliable optimal control solutions, which enables the nested formulation to find the same optimal design as the simultaneous formulation [2] and thus are mathematically equivalent. Note that an effective feasibility constraint in the outer loop usually leads to a more conservative search space. In addition, the nested structure changes the search direction. This means that the nested strategy may not be able to converge to the same optimal solution as the simultaneous formulation in some cases. Performance reduction due to the first factor can be improved by minimizing the approximation error of design spaces, if active constraints exist at the optimal design. The second factor is case-dependent and requires additional information to resolve. The feasibility constraints can only be generated case-by-case. In general, we only need to define feasibility constraints if existing constraints cannot lead to the identification of feasible inner-loop control trajectories.

One obvious yet trivial choice of feasibility constraint $G_F(\cdot)$ is the probability constraint. This formulation guarantees the equivalent design space. When the search direction and the algorithm does not inhibit the search of the optimal solution, the two formulations should result in the same optimal solution. Due to the fact that satisfaction of the reliability constraint in either loop and the symmetry of the nested co-design structure, it is not necessary to choose the probability constraint as the feasibility constraint unless exactness of design space is required.

Moreover, the current state-of-art RA methods can only provide reliability evaluation up to a certain accuracy level, so recovering the exact design space of the simultaneous RBCD for the nested RBCD is impractical.

As mentioned earlier in the reliability assessment discussion, the nested approach has the potential to increase the computational cost dramatically due to the increased number of iterations. However, system complexity is reduced for the decoupled sub-problems. By decoupling the optimal control design and reliability assessment from the original problem, there is enhanced flexibility in the choice of solution algorithm, and choosing a tailored algorithm for each sub-problem may produce a net benefit by reducing the cost of solving the inner loop. This is especially important when dealing with multidisciplinary problems. Solving the optimal control problem using DT can be very efficient with a quadratic objective and linear constraints (arising from linear dynamics). The efficiency and accuracy can be further improved with adaptive meshing strategies, where the continuous problem is only transcribed at a limited number of steps. Interested readers may refer to Chap. 4 of Ref. [34] for a deeper understanding of mesh refinement for direct optimal control.

3.3 Implementation Strategy. The nested co-design problem with reliability constraints is composed of three major elements: the system-level design optimization with respect to plant design

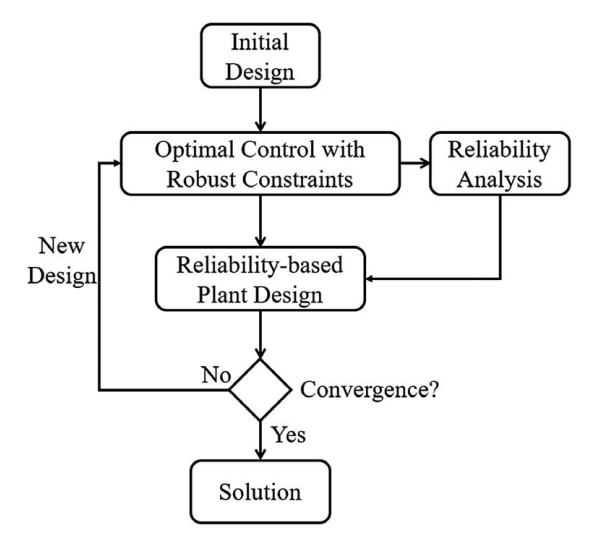


Fig. 1 Reliability-based nested co-design flowchart

variables (outer-loop problem), the optimal control design (inner-loop problem), as well as the reliability assessment (outer-loop, inner-loop, or both). If reliability constraints are enforced in the outer loop with the nested co-design problem formulation, the RBCD problem can be represented using a flowchart as shown in Fig. 1. Existing solvers can be used for each of these three elements depending on problem type, computational efficiency, and accuracy requirements. For example, the DT method can be used to solve the optimal control problem efficiently, while reliability analysis can be carried out using first-order reliability methods. The outer-loop plant design problem solver can also be selected based on the variable type, design space, and continuity of the problem.

The implementation of the reliability-based co-design problem with the above formulations could start with an initial design for the plant, generally in the feasible design space. The plant design can be optimized in the outer loop, with the optimal control for the candidate plant design information obtained by solving the inner-loop problem, while reinforcing the reliability constraints simultaneously. When using the nested co-design formulation, the plant design is held fixed for during both control design and reliability assessment in the inner-loop problem. The detailed steps of this process are as follows:

- (1) Initialize the plant design $\mu_{x_{p0}}$. For the common co-design problem formulation, the initial plant design can be identified in the feasible design region where a feasible controller design exists.
- (2) For the current plant design, solve the optimal control problem in the inner loop. The inner-loop probability constraints are moved to the outer loop, while approximated reliability constraints are added to the inner loop and make it deterministic.
- (3) Implement the reliability analysis for the outer loop probabilistic constraints, considering a robust optimal control design. If path constraints are present, forward integration can be used to generate the states of the controlled plant for all tested random samples. The sample results are then used for path reliability assessment by the chosen reliability analysis method.
- (4) Conduct the reliability-based plant design optimization, considering the optimal control and the assessed reliability.
- (5) Check convergence. If the process has not converged, a new candidate plant design will be proposed by the plant optimizer. Steps 2–4 are then repeated.

For the scenario with a nested co-design formulation that requires reliability analysis in both inner and outer loops, the computational expense could increase significantly, especially for the reliability analysis considering time-dependent control trajectories. While conducting the reliability analysis in both loops could ensure accuracy, it is impractical, however, for most realistic design applications due to its prohibitively high-computational costs. In addition, the combination of reliability analysis with inner-loop optimal control trajectories presents a significant challenge, as a time-dependent RBDO problem must be solved repeatedly for each co-design iteration.

From the perspective of formulation, having reliability constraints in both loops does inspire more applicable formulations. For instance, a practical formulation of nested RBCD is to convert the probabilistic constraints in one design loop (e.g., inner loop) to their deterministic approximations and retain the probabilistic constraints in the other design loop (outer loop), so that the computationally expensive reliability analysis need only to be conducted in one design loop. Note that replacing the probabilistic constraints in both loops leads to a robust nested co-design formulation, which is outside the scope of this paper. Similar to deterministic co-design problems, there are many choices of the deterministic approximations for probabilistic constraints. One possible choice could be a linear approximation of the worst-case constraint functional variation:

$$G_{j}\left(t, \boldsymbol{\xi}(t), \mathbf{x}_{c}(t), \boldsymbol{\mu}_{\boldsymbol{x}_{p}}\right) + \sum_{i=1}^{N} \eta_{i} \max\left(\frac{dG_{j}}{d\mu_{x_{pi}}} \sigma_{x_{pi}}\right)$$

$$\leq 0, j = 1, \dots, N_{c}$$

$$(16)$$

where *i* indicates the *i*th random variable of *N* variables. The max (\cdot) function determines the linear approximation of the worst function variation caused by design uncertainties. The product of the coefficient η_i and the standard deviation of random variable $\sigma_{x_{p_i}}$ can be used to account for plant design uncertainties in a deterministic manner for control design, and the values can generally be chosen based upon the confidence interval.

Since this probabilistic constraint simplification is only made to one of the design loops, tightening, or even some relaxation, of design constraints is allowable when using algorithms that accommodate intermediate constraint violations. For the RBCD problem using the nested design formulation with probabilistic constraints applied to both design loops, it is recommended to apply the stated deterministic approximation of probabilistic constraints to the inner-loop control design problem, since the computational cost of reliability analysis can be reduced significantly once the inner-loop design constraints become deterministic with respect to the design variables.

4 Reliability-Based Co-Design Case Studies

Three case studies are introduced in this section. The first case study (Case 1) is a simplified co-design problem, which can be viewed as the design of a static time-invariant system. In Case 1, the RBDO implementations with different co-design formulations are presented and compared. The second case study is a co-design problem involving a scalar dynamic system, with a constraint on the final state. Different reliability analysis methods are applied to the nested co-design formulation, with a comparison of convergence and computational efficiency characteristics of different random variable distributions and different target reliabilities. The third case study is a simplified wind turbine co-design problem involving optimal rotor control optimal lattice tower design. The results of deterministic nested co-design and a sensitivity study (with different levels of inner-loop relaxations for the reliability-based nested co-design) are presented.

4.1 Case Study 1: Static Co-Design Problem. As a tractable example to compare different problem formulations, this case study uses a modified bi-variate Matyas function as the objective function,

with two probability constraints that couple the scalar plant and control variables. The simultaneous formulation is

$$\min_{\mu_{x_p}, x_c} \quad 0.26(\mu_{x_p}^2 + x_c^2) + 0.48\mu_{x_p} x_c$$
subject to
$$Pr(x_p - 3x_c^{0.6} \le 0) \ge 0.95$$

$$Pr\left(\frac{x_c^2}{5} - x_p \le 0\right) \ge 0.95$$

$$0 \le \mu_{x_p} \le 3$$

$$0 \le x_c \le 3$$

where $x_p \sim \mathcal{N}(\mu_{x_p}, \sigma_{x_p}^2)$ is a random design variable and u represents a static (time-invariant) control variable. The above problem is a simple example of a static reliability-based co-design problem formulated as a simultaneous problem, which can be solved as a two-dimensional RBDO problem. Note that this problem only serves as a comparison for simultaneous RBCD, nested RBCD, and nested RBCD with either inner-loop only or outer-loop only reliability analysis. This is not necessarily appropriate for a dynamic system, but it helps provide insight into the formulations, including the nature of the bi-level structure of the nested formulation.

For the nested formulation, since both probability constraints are control-dependent, they should be included in the inner loop following the classical nested co-design formulation:

$$\min_{x_c} \quad 0.26(\mu_{x_p}^2 + x_c^2) + 0.48\mu_{x_p}x_c$$
subject to $Pr(x_p - 3x_c^{0.6} \le 0) \ge 0.95$

$$Pr\left(\frac{x_c^2}{5} - x_p\right) \le 0 \ge 0.95$$

$$0 \le x_c \le 3$$
(18)

where μ_{x_p} is assigned by the corresponding outer loop. As discussed in Sec. 2.2, a feasibility constraint can be added in the outer loop to guarantee the existence of a solution in the inner loop. The choice of feasibility constraint is case-dependent; yet, we can always choose the inner-loop constraint to be the trivial (yet redundant) option. If the reliability constraints are chosen as feasibility constraints for this problem, the corresponding outer loop can be formulated as

$$\min_{\mu_{x_p}} \quad 0.26(\mu_{x_p}^2 + x_{c*}^2) + 0.48\mu_{x_p} x_{c*}$$
subject to $Pr(x_p - 3x_{c*}^{0.6} \le 0) \ge 0.95$

$$Pr\left(\frac{x_{c*}^2}{5} - x_p \le 0\right) \ge 0.95$$

$$0 \le \mu_{x_n} \le 3$$
(19)

where x_{c^*} is obtained by solving the inner-loop problem for a value of μ_{x_c} designated by the outer loop.

Alternatively, the feasibility constraint can be chosen by replacing the limit state functions by their upper bounds, for example:

$$\min_{\mu_{x_p}} \quad 0.26 \left(\mu_{x_p}^2 + x_{c*}^2\right) + 0.48 \mu_{x_p} x_{c*}$$
subject to
$$\mu_{x_p} - 3x_{c*}^{0.6} + \epsilon_1 \le 0$$

$$\frac{x_{c*}^2}{5} - \mu_{x_p} + \epsilon_2 \le 0$$

$$0 \le \mu_{x_p} \le 3$$
(20)

where ϵ_i are lumped parameters that shift the limit state functions to their upper bounds. Unlike the previous formulation, we no longer need reliability analysis for the outer loop, which reduces the computational effort.

As discussed at the end of Sec. 3.3, a significant reduction in the computational effort can be achieved by converting the probability constraints in the inner loop to their deterministic approximations. Based on this, the forth formulation is

$$\min_{x_{c}} \quad 0.26 \left(\mu_{x_{p}}^{2} + x_{c}^{2}\right) + 0.48 \mu_{x_{p}} x_{c}$$
subject to
$$\mu_{x_{p}} - 3x_{c}^{0.6} + \epsilon_{1} \le 0$$

$$\frac{x_{c}^{2}}{5} - \mu x_{p} + \epsilon_{2} \le 0$$

$$0 \le x_{c} \le 3$$
(21)

where ϵ_i are lumped parameters that add robustness to the optimal control problem. Azad and Alexander-Ramos [16] used a similar strategy for adding robustness to inequality constraints of the simultaneous co-design problem, where they reasoned that the tolerance term can be determined as a function of the first-order approximation of the variations in constraint function evaluation. Here, the purpose of robust control is to compensate for the relaxation in the inner loop where the mean values of the design variables are used for the optimal control design. Without the tolerance term, the controller designed for the mean design variables would fail for the reliability-constrained outer loop when randomness-induced variations in limit functions violate the constraints. As discussed in Sec. 3, the conservative constraints should be close to the worst functional variation, for retaining a closely approximated design space. The linearly approximated variations of the constraints are simply the standard deviation, which is 0.316 for this problem. The conservative coefficients are chosen as [1.65, 1.65] accordingly, which result in $\epsilon_1 = 0.52$ and $\epsilon_2 = 0.52$.

For the choice of conservative coefficients, probability constraints should be used as upper bounds if an interior-point method is used in the outer loop. This should lead to a conservative plant design and an aggressive control strategy due to the relaxed (or the aggressively approximated) inner-loop constraints. The closer the approximated constraints are to the true probability constraints, the more the original feasible design space is preserved. If the violation of constraints is allowed for intermediate steps, we can also approximate the inner-loop constraints conservatively, which leads to a robust control strategy. A trade-off always exists between robustness and accuracy. Larger tolerance terms increase the robustness of the controller, which makes the outer loop easier to solve. On the other hand, the optimal solution may be close to the constraints, and conservative (large) coefficients may exclude the original optimal solution and lead to sub-optimality. The conservative coefficients used above were found analytically, which was possible because the confidence interval of a normalized distribution can be approximated as the confidence interval.

Due to the simplicity of the first case study, Monte Carlo simulation is used to reduce errors induced by the approximation-based reliability analysis. The deterministic constraints are evaluated 100,000 times for each reliability constraint. An interior-point method is employed as the solver, which incorporates a barrier function into its objective. For a starting point of $[x_{p0}, x_{c0}]^T = [2, 2]^T$, the convergence performance of the four methods is presented in Fig. 2 and summarized in Table 1.

The optimal solution of the deterministic problem is $[x_p, x_c]^T = [0, 0]^T$ at the intersection of the two constraints. Any uncertainty would cause the failure of the deterministic design. The simultaneous reliability-based co-design solution $[\mu_{x_p}, x_c]^T = [0.5270, 0.1731]^T$ is considered as the baseline design. For the nested formulations, since the inner-loop control problem is always solved first, intermediate designs would always activate the upper constraint first. Then, the conflict between the gradient descent direction and the feasibility gradients keeps the convergence trajectory close to the upper constraint. The nested co-design formulation with reliability analysis in both loops leads to the closest result to the baseline design. This agrees with previous analysis since it provides an accurate

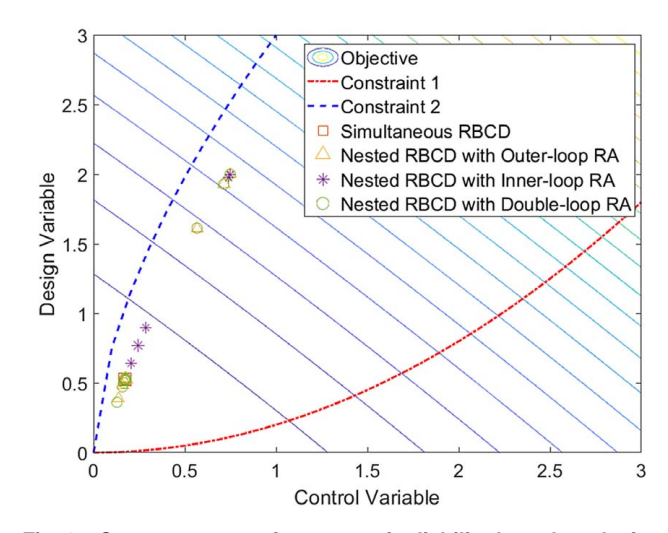


Fig. 2 Convergence performance of reliability-based co-design formulations

Table 1 Convergence history comparison for different formulations of the static co-design problem

Method	μ_{x_p}	x_c	Objective	Fcn evals
Simultaneous RBCD	0.5270	0.1731	0.1238	287
Nested RBCD with outer-loop RA	0.5289	0.1740	0.1248	52
Nested RBCD with inner-loop RA	0.7707	0.2453	0.2608	55
Nested RBCD with double-loop RA	0.5272	0.1731	0.1239	63

approximation of the feasible design space. However, it also requires the largest number of function evaluations across the three nested formulations, which is particularly expensive when MCS is employed. The solution produced by nested co-design with outer-loop reliability analysis is only slightly farther away from the strategy that has RA in both loops, with significantly fewer function evaluations. The converged optimum of the nested co-design with inner-loop reliability analysis is much farther away from the baseline, which indicates incoherence between the approximated design space and the original feasible design space. Note that an interior-point method is used for the outer-loop optimization, which limits the result of the nested formulations that use approximations to a combination of conservative plant designs and aggressive control designs. In addition, this demonstrates the flexibility of using a bi-level approach to tune the plant and control design, resulting in a feasible and near-optimal solution.

4.2 Case Study 2: Scalar Linear System. Consider the following simultaneous formulation of a co-design problem based on a scalar linear system:

$$\min_{\substack{\mu_{x_{p_1}}, \, \mu_{x_{p_2}} x_c(t), \, \xi(t)}} \frac{1}{2} \int_{t_0}^{t_f} x_c^2(t) dt + \frac{1}{2} c \xi^2(t_f)$$
subject to $Pr\{\xi(t_f) \leq \xi_{\max}\} \geq P_0$ (22)
$$\dot{\xi} = x_{p_1} \xi + x_{p_2} x_c$$

$$\xi(0) = \xi_0$$

where ξ is the scalar state, $x_c(t)$ is the control input, and ξ_{max} is the maximum allowed state value. The initial state $\xi(t_0)$ is specified. The plant design variables x_{p_1} and x_{p_2} are random design variables with the same distribution and c is a fixed parameter with value 1. The cost function has both running cost and terminal cost components. The problem is fixed-time free-end, which poses a probability

constraint on the final state. The upper simultaneous problem can be reformulated as a nested problem:

$$\min_{\mu_{x_{p_1}}, \, \mu_{x_{p_2}}} \frac{1}{2} \int_{t_0}^{t_f} x_{c*}^2(t) dt + \frac{1}{2} c \xi_*(t_f)^2$$
subject to $Pr\{\xi(t_f) \le \xi_{\max}\} \ge P_0$ (23)
$$\dot{\xi} = x_{p_1} \xi + x_{p_2} x_{c*}$$

$$\xi(0) = \xi_0$$

where $x_{c^*}(t)$ and $\xi_*(t_f)$ are the optimal control trajectory and the corresponding final state obtained by the inner loop:

$$\min_{x_{c}(t), \, \xi(t)} \frac{1}{2} \int_{t_{0}}^{t_{f}} x_{c}^{2}(t)dt + \frac{1}{2}c\xi(t_{f})^{2}$$
subject to
$$\dot{\xi} = \mu_{x_{p_{1}}}\xi + \mu_{x_{p_{2}}}x_{c}$$

$$\xi(0) = \xi_{0}$$
(24)

In this case, the inner loop is kept as the original deterministic optimal control problem. However, the inner loop is still intended for the satisfaction of the reliability constraint. The robustness is achieved solely via plant design. Note that this relaxation is valid here because the final state also appears in the objective function. It can be considered to be the penalty-based method, where the final state is minimized. The deterministic problem can be solved analytically by application of Pontryagin's maximum principle, which gives the following optimal trajectory and control:

$$\xi_{*}(t) = \xi(t_{0})e^{\mu_{x_{p_{1}}}(t-t_{0})} + \frac{\mu_{x_{p_{2}}}^{2}ce^{\mu_{x_{p_{1}}}(2t_{f}-t_{0}-t)}\xi(t_{0})}{2\mu_{x_{p_{1}}} - \mu_{x_{p_{2}}}^{2}c(1 - e^{2\mu_{x_{p_{1}}}(t_{f}-t_{0})}) \Big[e^{\mu_{x_{p_{1}}}(t_{f}-t)} - e^{\mu_{x_{p_{1}}}(t+t_{f}-2t_{0})}\Big]$$
(25)

and

$$x_{c*}(t) = \frac{2\mu_{x_{p_1}}\mu_{x_{p_2}}ce^{\mu_{x_{p_1}}(2t_f - t_0 - t)}\xi(t_0)}{2\mu_{x_{p_1}} - \mu_{x_{p_2}}^2c(1 - e^{2\mu_{x_{p_1}}(t_f - t_0)})}$$
(26)

For the nested formulation, the optimal control trajectory obtained from the inner loop is sent to the outer loop for RA, where the state trajectories of sampled plants are generated using numerical integration. The plant design variables are assumed to be normally distributed with a standard deviation of 0.1. The solution to the deterministic problem is [0.4586, 1.3980] for $\mu_{x_{p_1}}$ and $\mu_{x_{p_2}}$, which has a probability of failure of approximately 0.0934 (validated using MCS with a sample size of 100, 000). In addition to the deterministic results, the problem is also solved using MCS, AMV, and HL-RF methods. Five commonly used distributions (normal, lognormal, Weibull, Gumbel, and uniform) are used to test the robustness of different methods. In addition, a sensitivity study on the target reliability level and its effect on computational cost was also performed. The test results are summarized in Tables 2 and 3.

The MCS result is considered to be the baseline here. It is shown that the result of the AMV method is closest to the baseline result,

both in the plant and control design spaces. There is a deviation for the HL-RF method in the sense of the final state and control trajectory. Among the three tested methods, MCS requires a very large number of function evaluations, and therefore is not an efficient or practical method for reliability analysis. For all cases, the optimum obtained by the AMV method is closer to the MCS results than those of the HL-RF method, indicating that accuracy is an advantage of AMV. There is no divergence for the AMV or HL-RF methods for the cases with different distributions, so a robustness advantage of AMV is not evident. For efficiency, the AMV method requires fewer total iterations than the HL-RF method in most tested cases. It requires more iterations for lognormal distribution and when the target reliability is 0.99.

4.3 Case Study 3: Simplified Wind Turbine Co-Design Problem. A simplified wind turbine co-design problem is presented here where a two-dimensional lattice tower supports a horizontal-axis wind turbine, and a lumped-parameter aerodynamic model is used (Fig. 3). The plant design is the tower geometry, and the control design is parameterized as the time-varying axial induction factor (which in practice can be influenced by generator torque and pitch control). Plant design variables include tower height h, inner side length w_b of the square tube truss member, and the tube thickness t_b .

The two design objectives include maximizing energy production and minimizing tower cost. A path constraint limits the maximum tip deflection. The objective and constraints conflict since wind speed and energy potential generally increase with height (due to wind shear), but increased height (and tip thrust force) requires a stronger and more expensive tower. Meanwhile, control inputs of the turbine can mitigate excessive load, which provides an alternative to reduce the cost of energy. A sweet spot exists for a given cost model and wind profile where the total cost of energy is minimized. A lattice tower design is chosen instead of the popular tubular towers for the purpose of reducing material and installation cost for small-scale systems. Increasing height while maintaining a fixed cost generally results in increased structural deflections, but these are limited here by the path constraint on tip deflection mentioned earlier.

The simplified wind turbine model accounts for rotor aerodynamics and the tower structural dynamics. The well-known actuator disk model is used for aerodynamics (i.e., the air velocity at the disc is related to the free stream velocity $U_{\rm inf}$ and the axial induction factor a). The axial induction factor is essentially the relative change in the wind velocity from upstream to downstream. The power output and thrust force are also related to the axial induction factor. Here, we assume that the induction factor can be arbitrarily changed within the limits $0 \le a \le 1/3$. The largest physically meaningful value of this factor is a = 1/2, but maximum energy extraction occurs at a = 1/3. For the disk actuator model, the velocity at the disk U_d can be calculated as

$$U_d = U_{\inf}(1 - a) \tag{27}$$

The time-varying free stream velocity trajectory used here is based on the wind data acquired from Ref. [35]. The wind speed is modeled as a superposition of the mean wind speed (which varies with tower height) and a time-varying portion based on the first three Fourier modes of the referenced data. Specifically, it is

Table 2 Comparison among MCS, AMV, and HL-RF for Log-normal, Weibull, Gumbel, and Uniform distributions

	Lognormal (0,1)		Gumbel (0,1)		Weibull (1,1.5)		Uniform (-0.5,0.5)	
Method	$F, \mu_{x_{p_1}}, \mu_{x_{p_2}}$	Iteration	$F,\mu_{x_{p_1}},\mu_{x_{p_2}}$	Iteration	$F,\mu_{x_{p_1}},\mu_{x_{p_2}}$	Iteration	$F, \mu_{x_{p_1}}, \mu_{x_{p_2}}$	Iteration
MCS	5.73,0.58,1.4	64	5.77,0.59,1.4	64	5.76,0.59,1.4	64	5.88,0.6,1.4	64
AMV	6.8,0.72,1.4	364	5.24,0.48,1.34	339	4.65,0.4,1.35	245	4.56,0.41,1.4	245
HL-RF	4.85,0.40,1.04	204	5.77,0.4,1.01	320	5.79,0.4,1	322	5.81,0.4,1	325

Table 3 Comparison among MCS, AMV, and HL-RF for Normal distributions with different target reliability

Method	$P_0 = 0.9$		$P_0 = 0.95$		$P_0 = 0.99$	
	$F, \mu_{x_{p_1}}, \mu_{x_{p_2}}$	Iteration	$F,\mu_{x_{p_1}},\mu_{x_{p_2}}$	Iteration	$F,\mu_{x_{p_1}},\mu_{x_{p_2}}$	Iteration
MCS	5.76,0.58,1.4	64	5.78,0.59,1.4	63	5.78,0.59,1.4	64
AMV	4.7,0.4,1.36	245	4.78,0.4,1.31	309	5.37,0.4,1.36	354
HL-RF	5.8,0.40,1	322	5.78,0.4,1	322	5.76,0.4,1.01	320

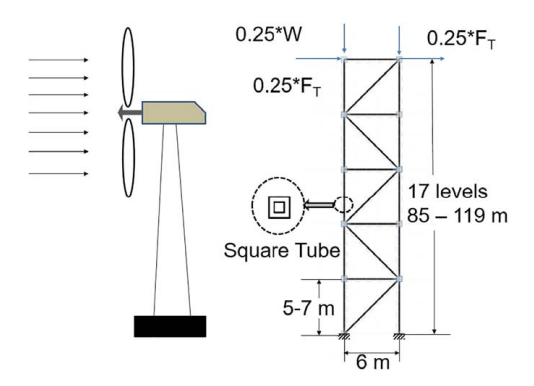


Fig. 3 Simplified lattice tower supported wind turbine

modeled as

$$U_{\inf}(t, h) = 5\left(\frac{h}{10}\right)^{0.17}$$

$$-6.77\cos 0.185t + 4.37\sin 0.185t + 0.874\cos 0.37t + 6.59\sin 0.37t + 4.81\cos 0.555t - 0.854\sin 0.555t$$
(28)

where t ranges from 0 to 24 hours. The corresponding power coefficient C_P and thrust coefficient C_T are defined as

$$C_P = 4a(1-a)^2, \quad C_T = 4a(1-a)$$
 (29)

 C_P can be rewritten as a function of C_T :

$$C_P = C_T \left(1 + \sqrt{1 - C_T} \right), \quad 0 \le C_T \le \frac{8}{9}$$
 (30)

allowing us to use the thrust coefficient as the control input instead of *a*. With the coefficients known, we can apply momentum theory to calculate the mechanical turbine power:

$$P = \frac{1}{2}\rho C_P A_b U_{\text{inf}}^3 \tag{31}$$

where A_b is the turbine swept area and ρ is air density (assumed to be 1.225 kg/m³ here). The thrust force at the turbine axis of rotation (tower tip) is

$$T = \frac{1}{2}\rho C_T A_b U_{\rm inf}^2 \tag{32}$$

Here, we assume the tower is composed of a fixed number of equal-height repeating mast sections, as shown in Fig. 3. The total tower height is treated as a continuous design variable. The structural dynamics of the tower is modeled using finite element analysis with a mesh having m movable nodes and 2m degrees of freedom, expressed in the following equation (after applying boundary conditions):

$$\mathbf{M}\ddot{\mathbf{x}} + \mathbf{C}\dot{\mathbf{x}} + \mathbf{K}\mathbf{x} = \mathbf{F}(t) \tag{33}$$

where $\mathbf{x} \in \mathcal{R}^{2m}$ represents the planar movement of all m non-fixed nodes. \mathbf{M} and \mathbf{K} are the $2m \times 2m$ global mass and stiffness matrices.

The forces on all nodes are expressed using the time-varying $2m \times 1$ vector $\mathbf{F}(t)$. Before applying boundary conditions (fixed base nodes), the stiffness matrix is singular, but after eliminating rows and columns corresponding to fixed (zero degrees of freedom) nodes, the stiffness matrix is symmetric positive definite. The corresponding state-space model is

$$\dot{\xi} = \begin{bmatrix} \mathbf{0} & \mathbf{I} \\ -\mathbf{M}^{-1}\mathbf{K} - \mathbf{M}^{-1}\mathbf{C} \end{bmatrix} \xi + \begin{bmatrix} \mathbf{0} \\ \mathbf{M}^{-1} \end{bmatrix} \mathbf{F}(t)$$
 (34)

The quantity $\xi \in \mathcal{R}^{4m}$ is the augmented state variable vector composed of both position and velocity states, i.e., $\xi^T = [\mathbf{x}^T, \dot{\mathbf{x}}^T]$. The system model used here does not approximate physical damping. Real structures do have internal damping, and here, an approximate damping term is added for numerical stability. Here, we assume the damping matrix is a linear combination of the mass and stiffness matrices [36]:

$$\mathbf{C} = \gamma_1 \mathbf{K} + \gamma_2 \mathbf{M} \tag{35}$$

where γ_1 and γ_2 are damping coefficients. The damping ratio κ is defined as a function of damping coefficients and the natural frequency. It is expressed as

$$\kappa = \frac{\gamma_1}{2\omega_n} + \frac{\gamma_2 \omega_n}{2} \tag{36}$$

where ω_n represents a natural frequency of the tower. Substituting ω_n with the first modal frequency of the tower and the damping ratio with a designated value, the system of equations can be solved for corresponding γ_1 and γ_2 values.

For the inner loop of the optimal control problem, the variable is the thrust coefficient trajectory $C_T(t)$, which is constrained to remain between 0 and $\frac{8}{9}$ throughout the time horizon. The inner loop is solved using the DT method (see Sec. 2). A MATLAB-based toolbox for solving linear-quadratic dynamic optimization problems [23,24] is used as the solver. To solve higher-order problems with nonlinear dynamics, it is recommended to use nonlinear direct optimal control packages, such as GPOPS II, which have built-in mesh refinement and automatic differentiation algorithms for an efficient and accurate solution.

The energy production revenue is calculated based on the price of electricity (0.12 USD/kWh) and the expected service life (20 years). The tower cost is estimated using a material mass cost (3.0 USD/kg) and an approximate construction cost (10 times the material cost). Operating expense is not included in this simplified model. The Pareto front was obtained using the ϵ -constraint method, which is presented in Fig. 4. Here, ϵ is chosen as the tower cost changing between the minimum tower cost and the maximum tower cost determined by the variable boundaries. About 30 points are picked and spaced uniformly; the resulting Pareto front illustrates the tradeoff between (approximate) energy revenue and tower cost. After the following discussion of the deterministic multiobjective problem, the deterministic and reliability-based co-design problems are solved for a fixed tower cost. In addition, a parametric study on the estimated robustness term of the inner-loop inequality constraint is also conducted.

The objective function axes displayed in Fig. 4 are normalized using the maximum possible tower cost (based on plant variable bounds), 4.236×10^7 , and energy revenue based on the maximum

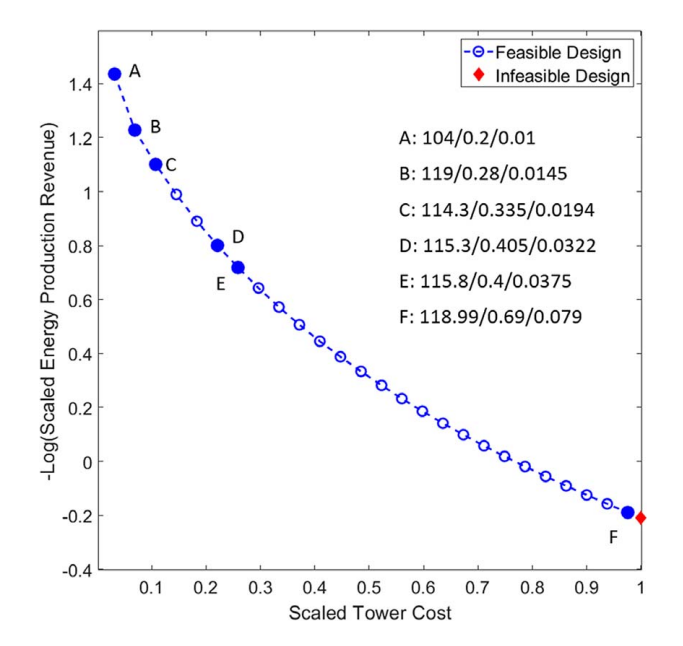


Fig. 4 Pareto front of the deterministic wind tower co-design problem, numerical values correspond to $h/w_b/t_b$

wind speed and a thrust coefficient of 16/27, which is 3.128×10^7 . The increasing tower cost leads to infeasible designs as the tower height approaches $119\,\mathrm{m}$, since the cross-sectional variables both approaches the upper limits. Also, we observe non-monotonic behavior of cross-sectional geometry at points C and E. This could be a result of relaxing the tower height as a continuous variable. Lattice towers are usually repeated stacks of mast sections, which should be an integer. By setting the total number of levels fixed, we are able to make the tower height a continuous variable.

For two consecutive points on the Pareto front, an increase in height may lead to a more rapid decrease in stability, which takes a much larger thickness and therefore even smaller side length of the cross section to compensate. For optimal designs between C and D, E and F, both side length and thickness grow simultaneously as the height increases.

Consider a case where the tower cost is fixed at 2.5×10^6 , the height range is constrained between 85 m and 119 m, and the member section geometry bounds are tightened to [0.2, 0.3] m (side length) and [0.02, 0.03] m (side thickness). The purpose of this modification is to reduce the range of these two degrees of freedom such that observation of the trade-offs between control trajectory and height can be made. In addition, different robustness terms have been tested, the results are summarized in Table 4 and Fig. 5.

Comparing with the deterministic co-design results, which takes an aggressive control trajectory for a shorter (yet stronger) tower, RBCD-based designs all converge very closely to $[h, w_b, t_b]^T = [110, 0.2, 0.02]^T$. The converged plant design results do not depend upon the choice of robustness terms in the inner-loop control problem. Alternatively, a large robustness term results in a more conservative control in the inner loop. The conservative control in the inner loop leads to sub-optimal design at the system

Table 4 Tower design results of the wind turbine co-design problem

Method	h	w_b	t_b	Energy revenue
Co-design	95.67	0.2106	0.021	3.54e9
RBCD(10%)	110.08	0.2	0.02	5.08e7
RBCD(30%)	110.8	0.2	0.02	5.08e7
RBCD(50%)	110.03	0.2	0.02	4.92e7
RBCD(70%)	110.08	0.2	0.02	4.91e7

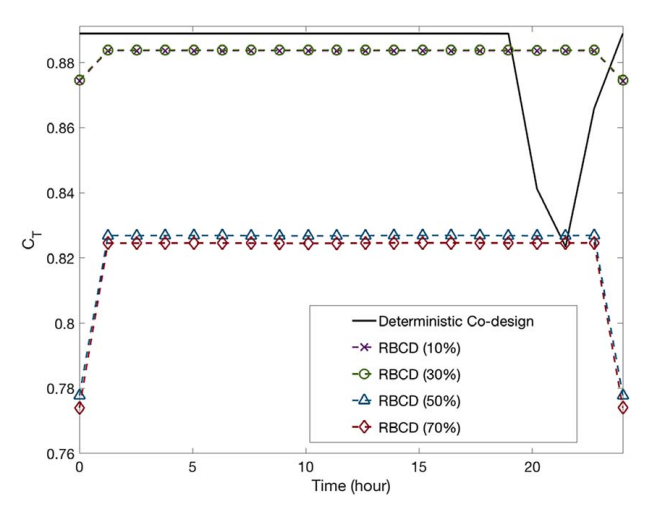


Fig. 5 Control trajectory of deterministic and reliability-based co-design

level, which agrees with the discussion in Sec. 3. However, this change of control design space does not affect the plant design space much, leading to the observed behavior where the RBCD cases all converge closely in the outer loop.

5 Discussion and Conclusion

In this work, a comparative study of RBCD problem has been conducted for different formulations and algorithms, where the co-design problem is integrated with the reliability-based design optimization framework for an optimal system design and a corresponding control trajectory that satisfies all reliability constraints pertaining to plant design uncertainties. The RBCD problem is decomposed in a nested manner, with robust optimal control and reliability assessment performed in the inner and outer loops, respectively. Plant and control design changes can work together synergistically to provide a more robust design under aleatory uncertainties. Numerical and application-based examples are presented to provide an in-depth discussion of the different problem formulations, accuracy and efficiency comparison of different reliability assessment strategies, implementation challenges, as well as strategies for feasible relaxations.

In particular, a reformulation based on the directly incorporated nested co-design and reliability-based design optimization is provided, which relaxes the soft constraints of the optimal control design problem such that the nested RBCD problem can be solved more efficiently. The efficacy and trade-offs are discussed and shown through analysis and case studies. It shows that the reformulated nested RBCD problem simplifies the process of solving the reliability-based optimal control problem but can still converge to a feasible solution with respect to the original reliability constraints. However, the nested RBCD would converge to the same optimal solution as the simultaneous RBCD when the original probabilistic constraints can be accurately approximated in the inner-loop design problem.

The current RBCD framework is demonstrated for reliability-constrained co-design problems with quadratic objectives, linear dynamics, and plant parameter uncertainties. However, the framework can be extended to problems with higher-order objectives and nonlinear constraints by employing SQP methods with mesh refinement. Likewise, a surrogate-model-based adaptation can be made by implementing a sample-based modeling problem on top of the current framework. In both cases, the efficacy complies with a trade-off between accuracy and efficiency. For a more general co-design problem with uncertainties, other sources of uncertainties, such as stochastic loading, measurement noise, and model uncertainties, may exist. The proposed framework cannot

be applied directly in such cases due to the optimal control of the stochastic process, incomplete information, as well as unmodeled dynamics. These topics are considered future developments of RBCD.

As indicated at the end of Sec. 2.2, the state-of-art co-design strategy mainly focuses on OLC problems. This certainly does not withhold its capability of advanced control strategies. For example, model predictive control, which iteratively solves the open-loop optimal control problem with a receding time window, is an ideal candidate for short period control with known nonlinear dynamics. Since the inner loop of the proposed nested structure solves a fixed-time problem. It is a worthwhile future work to adopt different control strategies for different co-design problems, in particularly in the presence of different types of uncertainties.

In order to expand the current formulation to more general problems with different types of uncertainties, the modification for cases with loading uncertainties and model uncertainties and their effects on general dynamics should be investigated. Meanwhile, an accurate and efficient estimation of the robustness term in the relaxed nested structure would help to improve the robustness and efficiency of the nested RBCD strategy. In addition, RBCD can be viewed as a special class of time-dependent reliability-based multidisciplinary design optimization problems. Accordingly, an exploration of state-of-the-art time-dependent RBDO methods and uncertainty-based multidisciplinary design optimization methods would be a worthwhile effort.

Acknowledgment

This research has been supported partially by the National Science Foundation (NSF) (Funder ID:10.13039/501100008982) through the Faculty Early Career Development (CAREER) award (CMMI-1813111) and the Engineering Research Center (NSF ERC) for Power Optimization of Electro-Thermal Systems (POETS) with cooperative agreement EEC-1449548. The first author would like to acknowledge Dr. Daniel R. Herber for his help in the implementation of horizontal-axis wind turbine co-design case study.

References

- Allison, J. T., and Herber, D. R., 2014, "Multidisciplinary Design Optimization of Dynamic Engineering Systems," AIAA J., 52(4), pp. 691–710.
- [2] Fathy, H. K., Reyer, J. A., Papalambros, P. Y., and Ulsoy, A. G., 2001, "On the Coupling between the Plant and Controller Optimization Problems," Proceedings of the 2001 American Control Conference, Arlington, VA, June 25–27, Vol. 3, pp. 1864–1869.
- [3] Fathy, H. K., Papalambros, P. Y., Ulsoy, A. G., and Hrovat, D., 2003, "Nested Plant/Controller Optimization Wth Application to Combined Passive/ Active Automotive Suspensions," Proceedings of the 2003 American Control Conference, Denver, CO, June 4–6, IEEE, pp. 3375–3380.
- [4] Yan, H.-S., and Yan, G.-J., 2009, "Integrated Control and Mechanism Design for the Variable Input-Speed Servo Four-Bar Linkages," Mechatronics, 19(2), pp. 274–285.
- [5] Allison, J. T., 2013, "Plant-Limited Co-Design of An Energy-Efficient Counterbalanced Robotic Manipulator," ASME J. Mech. Des., 135(10), p. 101003.
- [6] Allison, J. T., Guo, T., and Han, Z., 2014, "Co-Design of An Active Suspension Using Simultaneous Dynamic Optimization," ASME J. Mech. Des., 136(8), p. 081003.
- [7] Deshmukh, A. P., and Allison, J. T., 2016, "Multidisciplinary Dynamic Optimization of Horizontal Axis Wind Turbine Design," Struct. Multidiscipl. Optim., 53(1), pp. 15–27.
- [8] Tu, J., Choi, K., and Park, Y., 1999, "A New Study on Reliability- Based Design Optimization," ASME J. Mech. Des., 121(4), pp. 557–564.

- [9] Youn, B., Choi, K., and Park, Y., 2003, "Hybrid Analysis Method for Reliability-Based Design Optimization," ASME J. Mech. Des., 125(2), pp. 221–232.
- [10] Youn, B. D., Choi, K. K., and Du, L., 2005, "Enriched Performance Measure Approach for Reliability-Based Design Optimization," AIAA J., 43(4), pp. 874–884.
- [11] Chiralaksanakul, A., and Mahadevan, S., 2005, "First-order Approximation Methods in Reliability-Based Design Optimization," ASME J. Mech. Des., 127(5), pp. 851–857.
- [12] Noh, Y., Choi, K., and Du, L., 2009, "Reliability-Based Design Optimization of Problems With Correlated Input Variables Using a Gaussian Copula," Struct. Multidiscipl. Optim., 38(1), pp. 1–16.
- [13] Liang, J., Mourelatos, Z., and Nikolaidis, E., 2007, "A Single-Loop Approach for System Reliability-Based Design Optimization," ASME J. Mech. Des., 129(12), pp. 1215–1224.
- [14] Nguyen, T., Song, J., and Paulino, G., 2010, "Single-Loop System Reliability-Based Design Optimization Using Matrix-Based System Reliability Method: Theory and Applications." ASME J. Mech. Des. 132(1), p. 011005
- Method: Theory and Applications," ASME J. Mech. Des., 132(1), p. 011005.
 [15] Du, X., and Chen, W., 2004, "Sequential Optimization and Reliability Assessment Method for Efficient Probabilistic Design," ASME J. Mech. Des., 126(2), pp. 225–233.
- [16] Azad, S., and Alexander-Ramos, M. J., 2018, "Robust MDSDO for Co-Design of Stochastic Dynamic Systems," ASME 2018 International Design Engineering Technical Conferences and Computers and Information in Engineering Conference (IDETC/CIE), Quebec City, Quebec, Canada, Aug. 26–29, p. V02AT03A002.
- [17] Park, H.-U., Lee, J.-W., Chung, J., and Behdinan, K., 2015, "Uncertainty-Based MDO for Aircraft Conceptual Design," Aircraft Eng. Aerosp. Technol., 87(4), pp. 345–356.
- [18] Liberzon, D., 2011, Calculus of Variations and Optimal Control Theory: A Concise Introduction, Princeton University Press, Princeton, NJ.
- [19] Deshmukh, A. P., Herber, D. R., and Allison, J. T., 2015, "Bridging the Gap Between Open-Loop and Closed-Loop Control in Co-Design: A Framework for Complete Optimal Plant and Control Architecture Design," 2015 American Control Conference (ACC), Chicago, IL, July 1–3, pp. 4916–4922.
- [20] Martins, J. R., and Lambe, A. B., 2013, "Multidisciplinary Design Optimization: A Survey of Architectures," AIAA J., 51(9), pp. 2049–2075.
- [21] Herber, D. R., and Allison, J. T., 2019, "Nested and Simultaneous Solution Strategies for General Combined Plant and Control Design Problems," ASME J. Mech. Des., 141(1), p. 011402.
- [22] Pontryagin, L. S., 1962, The Mathematical Theory of Optimal Processes, Interscience, New York.
- [23] Herber, D. R., 2017, "Advances in Combined Architecture, Plant, and Control Design". Ph.D. dissertation, University of Illinois at Urbana-Champaign, Urbana, IL.
- [24] Herber, D., Lee, Y., and Allison, J., n. d., DT QP Project, https://github.com/danielrherber/dt-qp-project
- danielrherber/dt-qp-project

 [25] Rahman, S., 2009, "Stochastic Sensitivity Analysis by Dimensional Decomposition and Score Functions," Probabilistic Eng. Mech., 24(3), pp. 278–287.
- [26] Hu, C., Youn, B. D., and Wang, P., 2019, Engineering Design Under Uncertainty and Health Prognostics, Springer, Cham, pp. 190–194.
- [27] Wu, Y., Millwater, H., and Cruse, T., 1990, "Advanced Probabilistic Structural Analysis Method for Implicit Performance Functions," AIAA J., 28(9), pp. 1663–1669.
- [28] Wang, Z., and Wang, P., 2013, "A New Approach for Reliability Analysis With Time-Variant Performance Characteristics," Reliability Eng. Syst. Safety, 115(1), pp. 70–81
- [29] Wang, Z., and Wang, P., 2012, "A Nested Extreme Response Surface Approach for Time-Dependent Reliability-Based Design Optimization," ASME J. Mech. Des., 134(12), p. 121007.
- [30] Wang, P., Wang, Z., and Almaktoom, A. T., 2014, "Dynamic Reliability-Based Robust Design Optimization With Time-Variant Probabilistic Constraints," Eng. Optim., 46(6), pp. 784–809.
- [31] Hu, Z., and Mahadevan, S., 2016, "A Single-Loop Kriging Surrogate Modeling for Time-Dependent Reliability Analysis," ASME J. Mech. Des., 138(6), p. 061406
- [32] Singh, A., Mourelatos, Z. P., and Li, J., 2010, "Design for Lifecycle Cost Using Time-Dependent Reliability," ASME J. Mech. Des., 132(9), p. 091008.
- [33] Hagen, Ø., and Tvedt, L., 1991, "Vector Process Out-Crossing As Parallel System Sensitivity Measure," J. Eng. Mech., 117(10), pp. 2201–2220.
- [34] Betts, J. T., 2010, Practical Methods for Optimal Control and Estimation Using Nonlinear Programming, Vol. 19, SIAM Press, Philadelphia, PA.
- [35] Jager, D., and Andreas, A., 1996, NREL National Wind Technology Center (NWTC): M2 Tower; Boulder, Colorado (Data). NREL Report DA-5500-56489.
- [36] Alipour, A., and Zareian, F., 2008, "Study Rayleigh Damping in Structures: Uncertainties and Treatments," The 14th World Conference on Earthquake Engineering, Beijing, China, Oct. 12–17.